EUMETSAT Satellite Application Facility on Climate Monitoring

Algorithm Theoretical Baseline Document

Meteosat Daylight Climate Data Set
DAL

DOI:10.5676/EUM_SAF_CM/DAL_MVIRI_SEVIRI/V001

DAL_SEVIRI_DS **CM-109**

DAL_MVIRI_DS **CM-110**

Reference Number: SAF/CM/DWD/ATBD/DAL
Issue/Revision Index: 1.2
Date: 28.03.2013

Document Signature Table

	Name	Function	Signature	Date
Author	Richard Müller, Jörg Trentmann	CM-SAF scientists		25/04/2012
Editor	Rainer Hollmann	Science Coordinator		25/04/2012
Approval	Rainer Hollmann	Science Coordinator		25/04/2012
SG Approval	SG	CM-SAF Steering Group		16/04/2013
Release	Martin Werscheck	Project Manager		16/04/2013

Distribution List

Internal Distribution	
Name	No. Copies
DWD Archive CM-SAF Team	1 1

External Distribution		
Company	Name	No. Copies
PUBLIC		1

Document Change Record

Issue/ Revision	Date	DCN No.	Changed Pages/Paragraphs
1.0	25/10/2011	SAF/CM/DWD/ATBD/DAL	Version presented to PCR-4 review
1.1	25/04/2012	SAF/CM/DWD/ATBD/DAL	Implement of changes due to PCR-4 review
1.2	28.03.2013	SAF/CM/DWD/ATBD/DAL	Editing and update after DRI7 Closeout

Applicable Documents

Reference	Title	Code
AD 1	CM-SAF Product Requirements Document	SAF/CM/DWD/PRD/2.1

Reference Documents

Reference	Title	Code
RD.1	ATBD Meteosat (MVIRI) Climate Data Set of SIS,SID and CAL : MVIRI_HEL	SAF/CM/DWD/PUM/MVIRI_HEL/1.1

Table of Contents

Table of Figures

1 The EUMETSAT SAF on Climate Monitoring (CM SAF)

The importance of climate monitoring with satellites was recognized in 2000 by EUMETSAT Member States when they amended the EUMETSAT Convention to affirm that the EUMETSAT mandate is also to “contribute to the operational monitoring of the climate and the detection of global climatic changes". Following this, EUMETSAT established within its Satellite Application Facility (SAF) network a dedicated centre, the SAF on Climate Monitoring (CM SAF, http://www.cmsaf.eu).
The consortium of CM SAF currently comprises the Deutscher Wetterdienst (DWD) as host institute, and the partners from the Royal Meteorological Institute of Belgium (RMIB), the Finnish Meteorological Institute (FMI), the Royal Meteorological Institute of the Netherlands (KNMI), the Swedish Meteorological and Hydrological Institute (SMHI), the Meteorological Service of Switzerland (MeteoSwiss), and the Meteorological Service of the United Kingdom (UK MetOffice). Since the beginning in 1999, the EUMETSAT Satellite Application Facility on Climate Monitoring (CM SAF) has developed and will continue to develop capabilities for a sustained generation and provision of Climate Data Records (CDR’s) derived from operational meteorological satellites.
In particular the generation of long-term data sets is pursued. The ultimate aim is to make the resulting data sets suitable for the analysis of climate variability and potentially the detection of climate trends. CM SAF works in close collaboration with the EUMETSAT Central Facility and liaises with other satellite operators to advance the availability, quality and usability of Fundamental Climate Data Records (FCDRs) as defined by the Global Climate Observing System (GCOS). As a major task the CM SAF utilizes FCDRs to produce records of Essential Climate Variables (ECVs) as defined by GCOS. Thematically, the focus of CM SAF is on ECVs associated with the global energy and water cycle.

Another essential task of CM SAF is to produce data sets that can serve applications related to the new Global Framework of Climate Services initiated by the WMO World Climate Conference-3 in 2009. CM SAF is supporting climate services at national meteorological and hydrological services (NMHSs) with long-term data records but also with data sets produced close to real time that can be used to prepare monthly/annual updates of the state of the climate. Both types of products together allow for a consistent description of mean values, anomalies, variability and potential trends for the chosen ECVs. CM SAF ECV data sets also serve the improvement of climate models both at global and regional scale.
As an essential partner in the related international frameworks, in particular WMO SCOPE-CM (Sustained COordinated Processing of Environmental satellite data for Climate Monitoring), the CM SAF - together with the EUMETSAT Central Facility, assumes the role as main implementer of EUMETSAT’s commitments in support to global climate monitoring. This is achieved through:

- Application of highest standards and guidelines as lined out by GCOS for the satellite data processing,
- Processing of satellite data within a true international collaboration benefiting from developments at international level and pollinating the partnership with own ideas and standards,
- Intensive validation and improvement of the CM SAF climate data records,
- Taking a major role in data set assessments performed by research organisations such as WCRP (World Climate Research Program). This role provides the CM SAF with deep contacts to research organizations that form a substantial user group for the CM SAF CDRs,
- Maintaining and providing an operational and sustained infrastructure that can serve the community within the transition of mature CDR products from the research community into operational environments.

A catalogue of all available CM SAF products is accessible via the CM SAF webpage, www.cmsaf.eu. Here, detailed information about product ordering, add-on tools, sample programs and documentation is provided.

2 Introduction

Long time series are needed for climate monitoring and analysis. Thus, there is a need to employ satellite information of the first generation of Meteosat satellites (Meteosat-2 to Meteosat-7) to generate information about climate. The MVIRI instruments on board the Meteosat First Generation satellites are equipped with 3 channels: a broadband channel in the visible, a channel in the Infrared, and a water vapour channel.

The second generation of Meteosat satellites is equipped with the Spinning Enhanced Visible and InfraRed Imager (SEVIRI) and the Geostationary Earth Radiation Budget (GERB) instrument. The GERB instrument is a visible-infrared radiometer for earth radiation budget studies. It provides accurate measurements of the shortwave (SW) and longwave (LW) components of the radiation budget at the top of the atmosphere. SEVIRI employs twelve spectral channels, which provide more information of the atmosphere compared to its forerunner. Several retrieval algorithms have been developed in order to use the additional information gained by the improved spectral information of MSG mainly for now-casting applications. However, these algorithms can not be applied to the MVIRI instrument on board the Meteosat First Generation satellites as they use spectral information that is not provided by MFG (NWC SAF cloud algorithm, CM-SAF radiation algorithm).

MVIRI is a passive imaging radiometer with three spectral channels a visible channel covering 500-900 nm, and infra-red channel covering 5.7-7.1 microns and 10.5-12.5 microns. MVIRI comes with a spatial resolution of 2.5 km for the visible and 5km for the IR channels, sub-satellite point respectively.

Hence, in order to be able to provide a long time series covering more than 20 years there is a need for a specific climate algorithm that can be applied to the satellites from the Meteosat First and Second Generation. Moreover, the retrieved climate variable must have climate quality.

The MAGICSOL (MAGIC SOLar irradiance) method, a combination of a climate Heliosat (HELIOSATellite) version (Hammer et al. 2003) and the Magic Global Irradiance Code – MAGIC (Mueller et al., 2009) does meet the above mentioned requirements. The method has been extended to provide daylight.

The applied MAGICSOL method needs only the broadband visible channel as satellite information and can therefore be applied to MFG and across different satellite generations. The application to other geostationary satellites, e.g., in the US and Asia is also possible. Hence, the MAGICSOL method has not only the power to provide long time series of ECVS, but also to provide ECVs, which cover the complete geostationary ring.

The Heliosat method, which is well established in the solar energy community, is the basis of the MAGICSOLs method for clouds. However, modifications of the original Heliosat method are needed to meet the requirements to generate a Climate Data Record and to provide Daylight (DAL). An outline of the MAGICSOLs method is given in section 4.1; the cloud and clear sky part are described in more detail in section 4.2 and section 4.2.2 respectively.

3 Algorithm Overview Daylight (DAL)

The solar surface irradiance consists of a diffuse fraction and a direct fraction. The diffuse fraction of the surface irradiance is defined as the solar radiation that has undergone scattering in the atmosphere. The direct irradiance is the solar flux reaching a horizontal unit of the earth's surface from the direction of the sun without being scattered. Both quantities are expressed in W/m². Daylight is the solar surface irradiance in the visible wavelength region (Figure 3–1, top) folded with the sensitivity of the human eye expressed as illuminance efficiency (Figure 3–1, bottom). The standard function established by the Commission Internationale de l'Éclairage (CIE, 1932) recently modified by Sharpe et al. (2005) is used for this purpose.

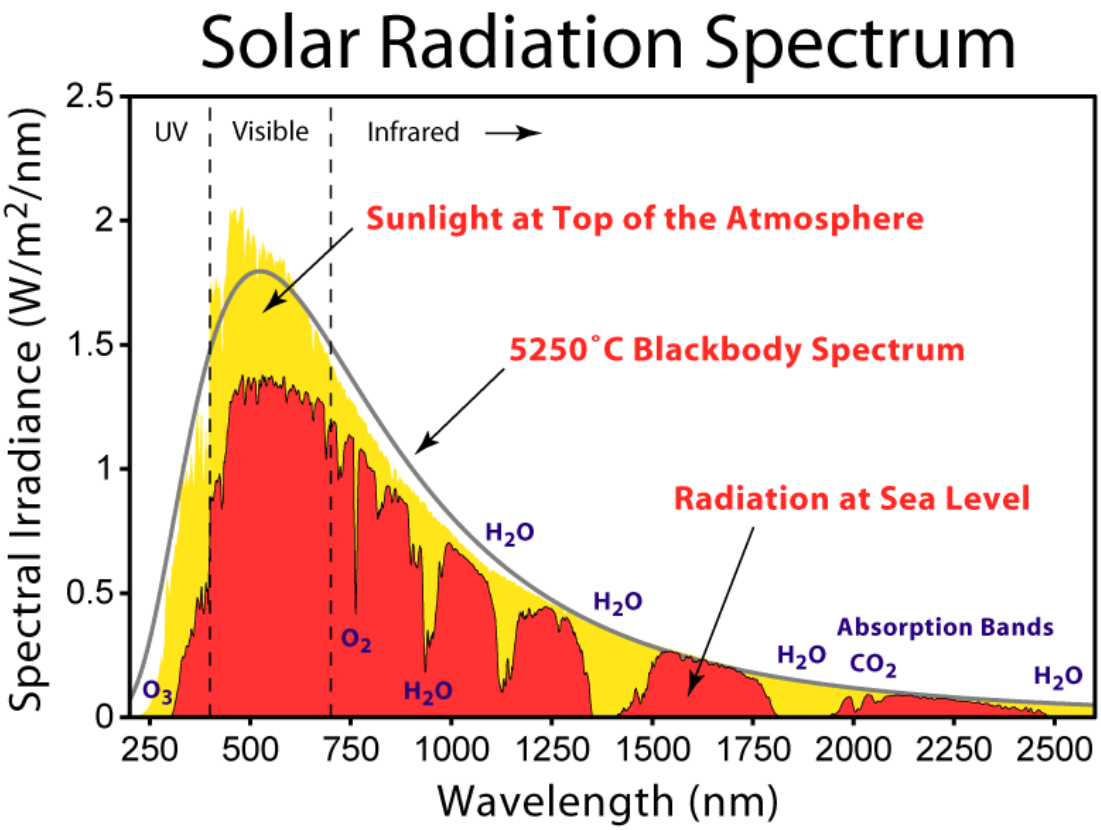

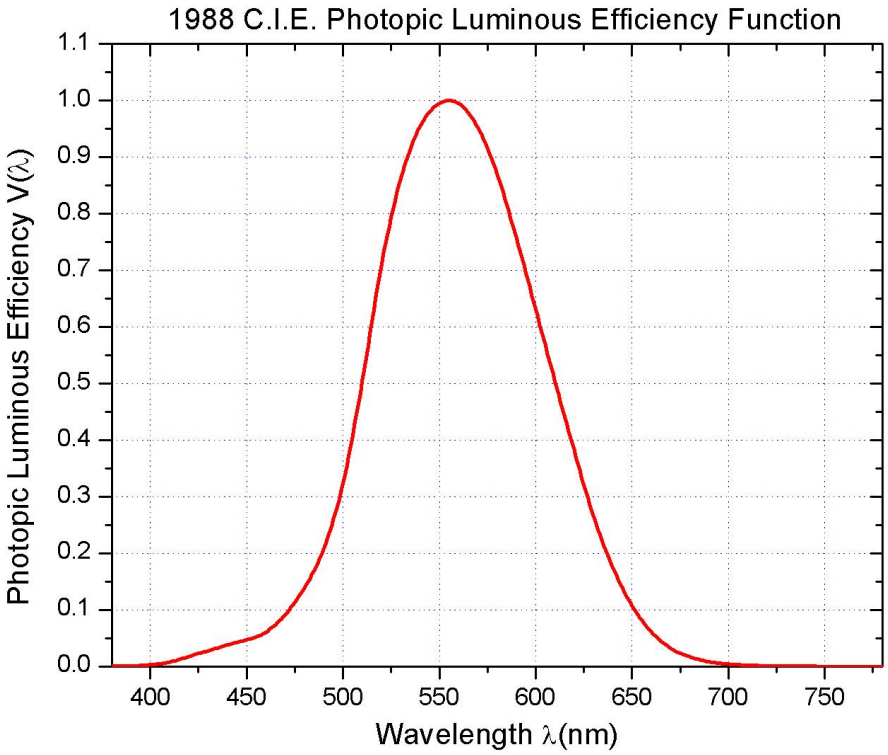

Figure 3–1: Solar spectrum containing the visible range (top) and illuminance efficiency (bottom).

The current interest in energy efficient design has led to a demand for methods of predicting daylight availability in buildings. For this purpose the amount of daylight on a horizontal plane is the important input information. More information on applications and user need are given at www.satelight.com and references therein. The analysis of seasonal affective disorder in order to support medicine as daylight is responsible for the generation of vitamin D and more general for climate monitoring. DAL will definitely be of use for the research in the Joint European Research Center, Ispra (JRC) and for the solar energy community in general (T. Huld personal communication).

In order to provide accurate information on daylight the MAGICSOL algorithm is applied.
The MAGICSOL method, a combination of a climate Heliosat version (Hammer et al. 2003) and the gnu-public license version of MAGIC (Mueller et al., 2009) does meet the above mentioned requirements. The method has been extended to provide daylight.
The MAGICSOL method needs the broadband visible channel as satellite information and can therefore be applied to MFG and across different satellite generations. The application to other geostationary satellites, e.g., in the US and Asia is also possible. Hence, the MAGICSOL method has not only the power to provide long time series of Meteosat based ECVs, but also to provide ECVs, which cover the complete geostationary ring.
The Heliosat method, which is well established in the solar energy community, is the basis of the MAGICSOLs method for clouds. However, modifications of the original Heliosat method are needed to meet the requirements to generate a Climate Data Record and to provide Daylight (DAL). An outline of the MAGICSOL method is given in section 4.1; the cloud and clear sky part are described in more detail in section 4.2 and section 4.2.2 respectively.

Figure 3–2 shows an overview of the algorithm and its interdependencies with other CM-SAF data sets.

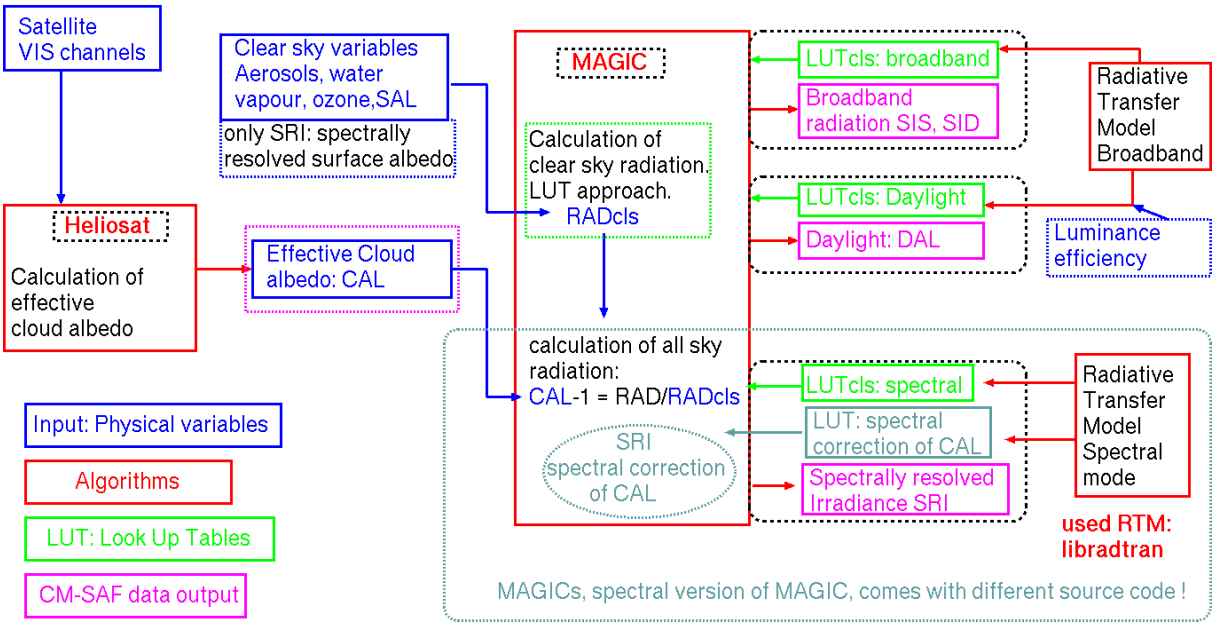

Figure 3–2: Functional diagram of the MAGICSOL algorithm for the calculation of daylight including independency with other CM-SAF radiation data sets. The retrieval of the effective cloud albedo is the basis input for all surface irradiance data sets. For the spectral resolved irradiance a spectral correction of the broadband effective cloud albedo is applied, which is not needed for daylight and broadband irradiance. The cores of the algorithms are the MAGIC algorithms. Dependent on the used Look-Up-Table MAGIC enables the calculation of broadband radiation and daylight. The MAGIC version for the spectral resolved irradiance MAGICs comes with the same approach concerning the physics, but the source code is optimised for the treatment of spectral bands and is therefore different to that of the broadband MAGIC code applied to derive daylight and broadband solar surface irradiance.

4 Theoretical Description

4.1 Physical Baseline

The pre-dominant dynamical effect on daylight is related to scattering and partly absorption on aerosol and cloud particles

The broadband cloud effect on daylight can be well defined with the effective cloud albedo derived with the established, accurate and fast MAGICSOL method (e.g. Posselt et al., 2011, MAGICSOL ATBD). The remaining issue is related to the estimation of the clear sky spectrum. The clear sky spectrum can be derived with a sophisticated Look-Up-Table (LUT) approach discussed in Mueller et al (2009).

A lookup table (LUT) is a data structure, used to replace a runtime computation with a simpler interpolation operation within discrete pre-computed results, see Figure 4–1 as an illustration. In our case pre-computed radiative transfer model (RTM) results contain the transmittance for a variety of atmospheric and surface states. Once the LUTs have been computed, the transmittance for a given atmospheric state can be extracted from the LUTs by interpolation for each satellite pixel and time. Finally, solar surface irradiance can be calculated from the transmittance by multiplication with the extra terrestrial incoming solar flux density. The idea behind the LUT approach for an irradiance retrieval scheme is to achieve equal accuracy as with the direct usage of an RTM, but without the need to perform RTM calculations for each pixel and time, thus leading to an improved computing performance.

The radiative transfer model libRadtran has been applied for the calculation of the basis look-up tables. LibRadtran is a collection of C and Fortran functions and programs for calculation of solar and thermal radiation in the Earth's atmosphere (A. Kylling and B. Mayer, http://

www.libradtran.org). It has (also) been validated by comparison with other models (Koepke et al. 1998, van Weele et al. 2000) and radiation measurements (Mayer et al. 1997)
LibRadtran offers the possibility of using the correlated-k approach of Kato et al. (1999). The correlated-k method is developed to compute the spectral transmittance (hence the spectral fluxes) based on grouping of gaseous absorption coefficients. The main idea is to benefit from the fact that the same value of the absorption coefficient k is encountered many times over a given spectral interval. Thus, the computing time can be decreased by eliminating the redundancy, grouping the values of k, and performing the transmittance calculation only once for a given value of k. 32 Kato bands are available in the solar spectrum. The basis LUT has been calculated for the 32 Kato bands, by application of the approach of Mueller et al. (2009) for each of the Kato wavelength bands.
In order to consider the cloud effect on DAL the well established Heliosat relations Hammer et al. (2003) are employed and adapted to the wavelength bands, which are outlined in the next paragraph, please see section 4.2 and 4.2.2 for further details.

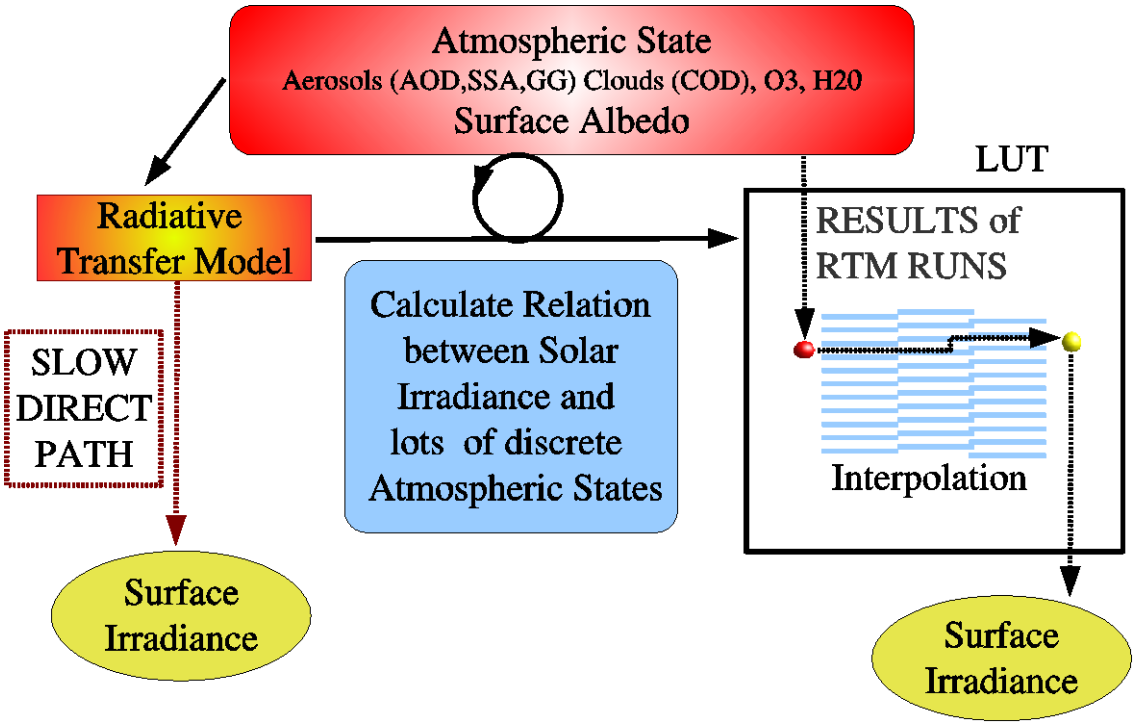

Figure 4–1: The relation of the transmission to a manifold of atmospheric states is pre-calculated with a radiative transfer model (RTM) and saved in a look-up table (LUT). Once, the LUT has been computed the transmittance for a given atmospheric state can be extracted from the LUT for each satellite pixel and time.

Relation of effective cloud albedo to solar irradiance:
The relation between the effective cloud albedo (CAL) and daylight (DAL) is predominantly given by:

$$DAL = DAL_{cls} * (1 - CAL) \qquad \text{Eq. 4-1}$$

Here DAL_{CLS} is the daylight for cloud free skies; the abbreviation “cls” denotes clear sky irradiance throughout the ATBD. CAL is the effective cloud albedo and describes the attenuation of daylight be clouds. The relation is evaluated in Janjai et al. (2003) and equals that given in Hammer et al. (2003) and Posselt et al. (2011) for solar irradiance. It is defined by physics, in detail by the law of energy conservation (Dagested, 2005).

The equation equals that for solar surface irradiance (Hammer et al., 2003) However, above a CAL value of 0.8 empirical corrections are needed as a consequence of the effect of optical thick convective clouds. The applied corrections are described in detail in section 4.2.2 and Hammer et al. 2003. With the knowledge of the effective cloud albedo, daylight can be derived by application of a clear sky model described in more detail in section 4.2.

4.2 Description of the Algorithm

4.2.1 Clear Sky model: The GNU-MAGIC approach for the retrieval of solar irradiance

The physical basis of the algorithm is described in Müller et al. (2009) and R. Müller et al. (2003). The MAGIC approach is applied to the visible spectral bands and used to retrieve the Daylight DAL by folding the derived irradiance in the visible with the illuminance efficiency. It combines the LUT approach for the calculation of the clear sky irradiances with the well established Heliosat relations (see section 4.2.2) for the consideration of the cloud effect. The MAGIC method for the retrieval of the daylight is described in this section, while in the following section the treatment of the cloud effect on the clear sky daylight is discussed.

The MAGIC code is based on the radiative transfer model calculations, following a look-up-table approach. The MAGIC code includes a basic clear-sky look-up-table (LUT), surface albedo map, water vapour climatology and aerosol climatology. The basic clear-sky LUT consists of radiative transfer model results for aerosols with different aerosol optical thickness, single scattering albedo, and asymmetry parameter. Fixed values for water vapour, ozone and surface albedo have been used for the calculation of the basis LUT: 15 kg/m^2 for water vapour column, 345 DU of ozone, and a surface albedo of 0.2. The basis LUT contains the results for all 32 Kato bands. The effect of the solar zenith angle on the transmission, hence the surface solar irradiance, is considered by the use of the Modified Lambert Beer (MLB) function (Mueller, 2004). The effects of variations in water vapour and surface albedo relative to the fixed values used in the calculation of the basis LUT might be corrected using the correction formulas and parameterizations.

However, it is important to note that water vapour and ozone does not affect the daylight significantly and the respective corrections applied to derive the broadband irradiance are obsolete, therefore. The databases in the MAGIC code can be updated and replaced with instantaneous measurements without changing the basic LUT and the code. Therefore the MAGIC code is fast, robust and suitable for operational algorithms.

The input parameters of the MAGIC code are date, time, solar zenith angle, latitude, longitude, effective cloud albedo (cloud index), fixed water vapour and ozone column density, aerosol optical thickness and single scatter albedo for aerosols. The output of the MAGICs code are the clear-sky and optionally the all sky solar irradiances in the 0.2-4.0 µm wavelength region, either the broadband sum or the spectral resolved irradiance. The asymmetry parameter for the aerosol scattering phase function is also fixed at 0.7 in the current version of the MAGIC code. The extra terrestrial total solar irradiance is 1366 W/m^2 and adjusted according to the earth-sun distance. The relation between the effective cloud albedo CAL and the all sky daylight DAL is already included in the MAGIC code. More details about the MAGIC code are described by Mueller et al. (2004, 2009)

The RTM libRadtran (Mayer and Kylling, 2005) was used for the generation of the basis LUT. RTM calculations were performed for the spectral bands between 350 and 1000 nm for numerous states of aerosols. Several types of aerosols were included (Hess et al., 1998). Increase in the computing performance has been achieved by the use of Modified Lambert Beer (MLB) functions (Müller et al., 2004) and the implementation of hybrid eigenvector LUTs (Müller et al., 2009). Relevant information on MAGIC needed for the description of DAL is taken from Müller et al (2009). The MLB relation works very well for the individual Kato bands as discussed in (Mueller et al., 2004).

Employing the MAGIC eigenvector hybrid LUT approach the clear sky daylight is calculated in a first step for the given atmospheric conditions and the respective wavelength region. The atmospheric conditions cover different values for aerosol optical depth, aerosol single scattering albedo and asymmetry parameter, and surface albedo.
Within the basic LUT the daylight for the actual aerosol state is derived by linear interpolation between the pre-calculated solar irradiance values associated to different aerosol states for fixed water vapour amount of 15 mm, an ozone content of 345 DU and a surface albedo of 0.2 for each wavelength band. Deviations in the surface albedo from the values assumed for the creation of the LUT are afterwards corrected by application Eq. 4-1

$$DAL_{CLS} = DAL_{CLS,\ LUT} * (0.98 + 0.1 * SAL) \qquad \textbf{Eq. 4-2}$$

Eq. 4-2 gives the correction of deviations in the surface albedo relative to the standard value used in the basis LUT. Here, *SAL* is the surface albedo and DAL_{LUT} is the Daylight retrieved from the LUT for the given aerosol state.

4.2.2 Treatment of the cloud effect

The broadband cloud transmission is calculated from the effective cloud albedo derived with the MAGICSOL method. The effective cloud albedo is defined as the normalised difference between the all sky and clear sky reflection in the visible observed by the satellite. The deviation of the actual reflection of the pixel from the clear sky reflection is a measure of the cloudiness. The brighter the pixel the more or thicker clouds are present. The effective cloud albedo is a measure of the cloud effect on the Earth's solar radiation budget.
The Heliosat algorithm uses reflection measurements given as normalized digital counts to determine the effective cloud albedo, also called cloud index (Cano et al., 1986; Beyer et al., 1996; Hammer et al., 2003). A clear sky model is used to calculate the solar surface irradiance based on the retrieved effective cloud albedo.
Basis of the Heliosat method are the rectified digital pixel counts of the visible Meteosat channel (High Resolution Visible). The respective data are called *"Rectified Image Data*" and provided by Eumetsat (EUM TD 06). No information from other channels is used. The first step in the Heliosat method is the retrieval of the effective cloud albedo (cloud index).

Thereby, the changes in the reflective properties of the clouds due to different insulation angles during the day and year are accounted for by a normalization with the sun elevation ($\cos(\Theta_z)$ - cosine of the sun's zenith angle) and a correction for the sun-earth distance f. Furthermore, the measured count value D is reduced by the dark offset D_0, which is a satellite specific value obtained by looking into dark space. Values below the dark offset are, thus, assumed to be zero.

$$\rho = \frac{D - D_0}{f \cos(\Theta_z)} \qquad \textbf{Eq. 4-3}$$

Here, D is the observed digital count including the dark offset of the satellite instrument. The dark offset does not arise from the Earth reflection but is an intrinsic instrument offset and has therefore to be subtracted. The effect of the sun-earth distance is considered by the factor *f*, finally, the cosine of the solar zenith angle corrects the different illumination conditions at the top of atmosphere introduced by different solar altitudes.
The effective cloud albedo is then derived from the normalized pixel count ρ, the clear sky reflection in counts ρ_{srf} and the albedo of a compact (not convective) cloud deck ρ_{max} by

$$n = \frac{\rho - \rho_{srf}}{\rho_{\max} - \rho_{srf}} \qquad \textbf{Eq. 4-4}$$

Here, ρ is the observed reflection in counts for each pixel and time. ρ_{sfc} is the clear sky

reflection in counts, which is a monthly value determined for every pixel separately. In principle this is done by using the reflection of the pixel in a cloud free case. This is usually the lowest occurring reflection during a certain time span (e.g., a month) derived for each pixel of the satellite image. $\rho_{\max}$ is the "maximum" cloud albedo. It could be determined in a similar fashion by choosing the "maximum" ρ per pixel and time span (Beyer et al., 1996) or by using a single value for the full disk that is dependent on the radiometer of the different satellites (Hammer et al., 2003). MAGICSOL follows the approach of Hammer et al. (2003) but a target region is used instead of the whole disk. One value of $\rho_{\max}$ is retrieved for each month, please see section 4.2.2.1 for further details.

The relation given in Eq. 4-5 between the effective cloud albedo CAL and the daylight DAL is evaluated in Janjai et al. (2003) and equals that given in Hammer et al. (2003) and Posselt et. al (2011) for solar irradiance.

$$DAL = DAL_{CLS} * (1-CAL) \qquad \textbf{Eq. 4-5}$$

This relation is defined by physics, in detail by the law of energy conservation (Dagested, 2005). However, above a CAL value of 0.8 empirical corrections are needed in order to consider:

- The effect of statistical noise, which could lead to CAL values above 1 and below 0 (occurs very seldom, however have to be considered).
- The effect of optical thick convective clouds.

In this intervals the CAL relation was determined from the statistical regression using the ground-based measurements of broadband irradiance at European sites and fitted to get the best performance at all the ground sites (Hammer et al. 2003 and references therein). It is assumed that the relations hold also for daylight. Eq. 4-6 provides the complete DAL-CAL relation for all possible CAL values. It is important to note that the empirical fit has been performed in the 80s and used since then without refitting. The RMSD of the empirical fit is 0.1.

$$\begin{aligned} CAL < -0.2,\ DAL &= 1.2 * DAL_{cls} \\ -0.2 < CAL < 0.8,\ DAL &= DAL_{cs*} (1-CAL) \\ 0.8 < CAL \leq 1.1,\ DAL &= DAL_{cls} * (2.07-3.67*CAL+1.67*CAL^2) \\ 1.1 < CAL,\ DAL &= 0.05 * DAL_{cls}. \end{aligned} \qquad \textbf{Eq. 4-6}$$

The source code of the method (Mesoscale Atmospheric Global Irradiance Code – MAGIC) was developed externally and is available under gnu-public license free of charge at http://sourceforge.net/projects/gnu-magic/.
Surface solar irradiance data sets derived with the Heliosat method and the Heliosat equations (Eq. 4-6) have been extensively validated against the ground-based solar radiation measurements (Perez et al., 2001; Wald et al., 2002; Meyer et al., 2003; Rigollier et al., 2004). It is well recognized that the surface solar irradiances derived from satellite measurements can be more accurate than that interpolated from the ground-based measurements, which are more than 30 kilometers apart (Perez et al., 1997; Zelenka et al., 1999). The validation results have demonstrated that the n-CAL relation is quite robust.

4.2.2.1 Auto calibration

For a climate data set homogeneity is an essential issue. Hence, there is a need for "calibration". In this section the auto-calibration method is described and evaluated.
The self-calibration algorithm is based on an operational determination of the "maximum" effective cloud albedo ρ_{max}. Input is sun zenith angle normalised counts corresponding to Eq. 4-3.
In analogy to Rigollier et al. (2002) a histogram of all available counts is generated.

However, instead of using an upper and a lower bound, only the 95%-percentile is used as self-calibration parameter and set to ρ_{max} (Hammer et al, 2003 and references therein).
However, the generation of the histogram for the full disk is rather slow due to the large pixel amount. Thus, a reduction of the considered region for the histogram was necessary. The selected region is located in the southern ocean between 15° W and 0° W and 58° S and 48° S. It features a high abundance of frontal systems with large cloud amounts most of the time, but hardly any convection.
A range of percentiles has been tested and the 95 percentile has been found to provide the best statistical stability. Using a percentile value and not the maximum of the histogram should exclude saturated pixels, which may have technical but no scientific reasons, and it also should exclude potential convective clouds. Depending on the applied method deep convective clouds might be useful for calibration, but they affect the stability of the 95 percentile applied within the MAGICSOL method.
The self-calibration algorithm is run at the 13 o'clock slot GMT which accounts for the slight westward shift of the region. The histogram is generated with a month worth of satellite data input. The resulting ρ_{max} is then applied for all slots within that month.
Figure 4–2 shows the temporal evolution of the normalized bias between the CM SAF data set and the BSRN data. The normalized difference is calculated as follows:
The arithmetic average over the complete time series of the BSRN and the satellite data is calculated for each station. The resulting mean difference (bias) is subtracted from all monthly means of the satellite data for each station. The mean difference (bias) over the covered time period is zero afterwards. However, **trends in the monthly differences are not affected by this normalization procedure**.
The differences between the monthly means of BSRN and satellite data are then averaged over all available stations, whenever monthly means from at least 3 stations are available. This leads to an overall time series of "normalized" differences of monthly means. This time series is then analysed for temporal trends. A trend in this time series would indicate in-homogeneities introduced by the self-calibration or the clear sky reflection maps (in counts). The applied method is necessary in order to avoid misleading trends in the monthly differences introduced by the quite different start and end points of the time series and the corresponding mismatch in the weighting of regional bias values. For the test of the self-calibration it is necessary to avoid artefacts due to local bias values as only the temporal evolution of the time series for the complete disk is of relevance. Contrary, the temporal evolution of the normalised mean monthly differences is not affected by the different numbers of available stations for certain months and their local bias.
As can be seen there is no detectable trend in the temporal evolution of the normalized monthly differences, which proves evidence of the homogeneity of the SIS time series. In contrast, the satellite raw counts show a significant and large trend, a decrease of the sensibility due to aging, see Figure 4–3. The absence of this trend in the normalized differences of the SIS data demonstrates the ability of the self-calibration method to correct for aging and satellite switches. It is worth noting that a statistically significant negative trend in the normalized differences is present in the GEWEX and ISCCP SIS data sets (Müller et al. 2011).

Because the Heliosat method is dedicated to retrieve the effective cloud albedo, a "clear sky" surface target has been not implemented for the self-calibration. Using a land surface target would introduce errors in the self-calibration method as the aging detected by observation of surface reflection is different to that detected with an appropriate cloud target. This is due to the stronger aging of optical devices in the UV and UV-near spectral regions, which leads to different rates of aging for the various land surface types (due to different spectral responses of the targets) in relation to clouds. Aging of "clear sky" reflection for any surface types is automatically accounted for by the retrieval of the planetary clear sky reflection (in counts) $\rho_{srf.}$

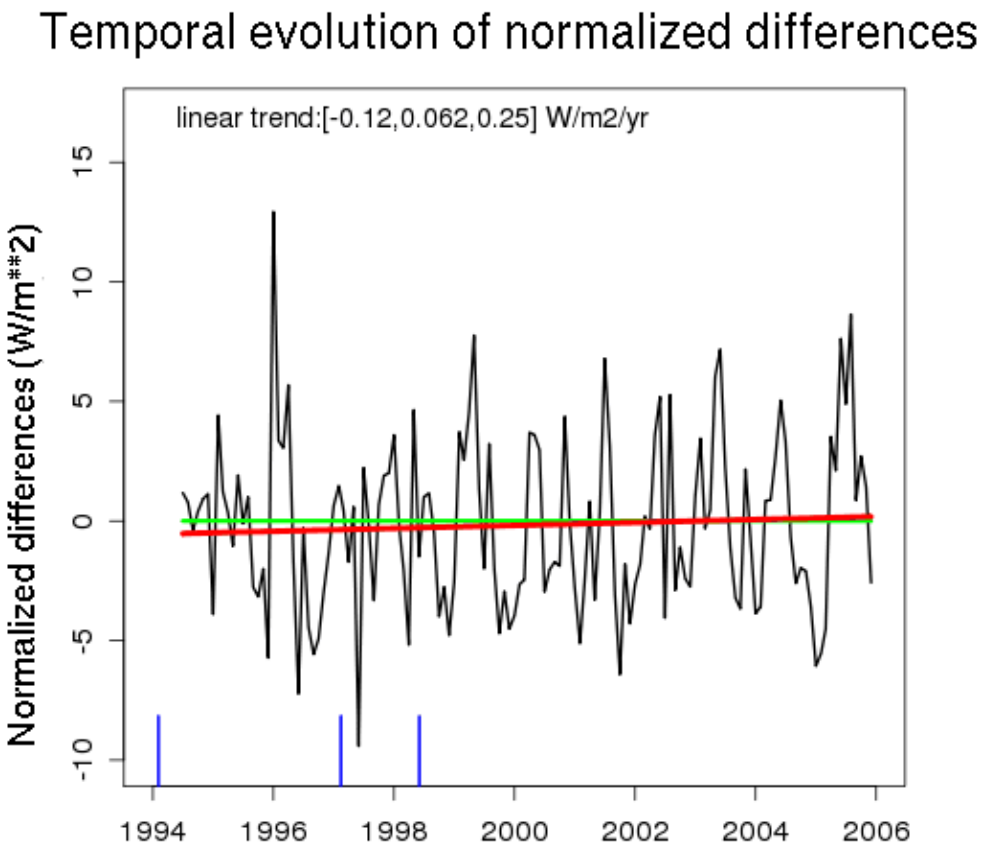

Figure 4–2: Temporal evolution of the normalized differences between the CM SAF data set and the BSRN data including the trend coloured in red. The trend is not significant, both concerning the statistical significance and the magnitude. The absence of a trend in relation to the large trends in the digital satellite counts demonstrates that the self-calibration works well.

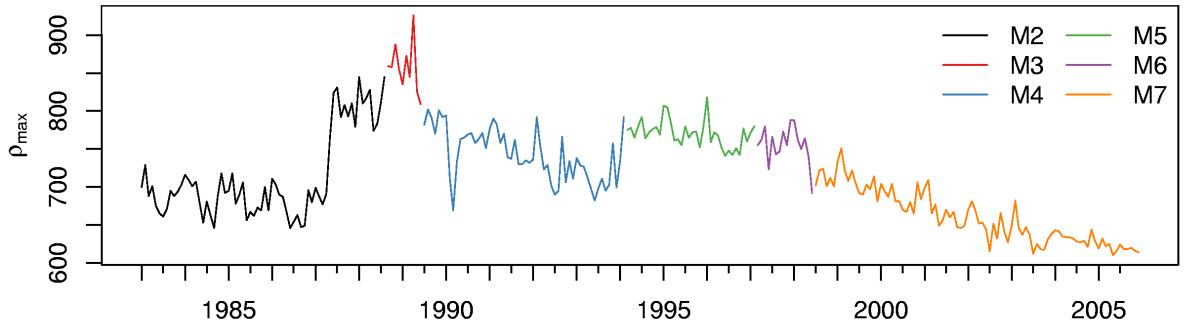

Figure 4–3: Time series of ρ_{max} from 1983 to 2006. The different colours are assigned to the different Meteosat satellites M2_M7 as given in the legend. Meteosat-1 data quality is to worse to be used for the data set. The jump around 1987 within the M2 time series is due to a gauge change of the instrument, performed by the EUMETSAT ground segment. The gauge jump has been well detected and corrected by the self-calibration method as well as the large instrument degradation given for Meteosat-7 (see validation report).

4.2.2.2 Clear sky reflection

The processing of the long time series of global radiation from Meteosat's first generation satellites employs a newly implemented clear sky or background reflection algorithm for Heliosat (Dürr and Zelenka, 2009). Instead of having a monthly constant field of the clear sky reflection ρ_{srf} in counts, a seven day running mean reflection field is used. Thus, sudden changes in the clear sky reflection due to, e.g., vegetation and snow are captured and represented faster than with the standard method. In addition, sudden jumps in the cloud index at month borders due to larger differences in the clear sky reflection fields are avoided.
The selection of a 7 day running mean is based on the publication by Zelenka (1999) where this time series approach has been introduced. It is justified with the persistence of weather patterns in the order of 5 to 7 days. However, problems with longer lasting overcast episodes phenomena as e.g. fog can occur and might lead errors in the cloud index retrieval.
The presented clear sky reflection algorithm is also able to detect snow and, thus, gives the opportunity to correct for some of the radiative properties of snow. The clear sky reflection is dominated by the surface reflection.

The algorithm to determine the clear sky reflection in counts ρ_{srf} is based on two tests that are applied to the TOA apparent reflection (ρ) in order to determine the evolution of ρ_{srf}. If both tests fail, i.e. if ρ is rather large as occurring in case of clouds and snow, ρ_{srf} is not changed.

$$\text{Test 1}: \left(\rho \le \rho_{srf} + \varepsilon_{up} \,\&\, \rho > \rho_{srf}\right) \left| \left(\rho < \rho_{srf} - \varepsilon_{low}\right) \rightarrow \rho_{srf} = \frac{6}{7}\rho_{srf} + \frac{1}{7}\rho \right.$$

(slow evolution)

$$\text{Test 2}: \left(\rho < \rho_{srf} \,\&\, \rho \ge \rho_{srf} - \varepsilon_{low}\right) \rightarrow \rho_{srf} = \frac{1}{2}\rho_{srf} + \frac{1}{2}\rho$$

(fast evolution)

$$\text{else}: \rightarrow \rho_{srf} = \rho_{srf}$$

(no change)

In contrast to Zelenka (2001), variable bandwidths ε_{up} and ε_{low} are employed, which were presented by Dürr and Zelenka (2009) with ρ_{max} being the satellite calibration constant, see

section 4.2.2.1.

$$\varepsilon_{up} = 0.125\rho_{\max} + \frac{8\left(\rho_{srf} - 0.15\rho_{\max}\right)}{0.25\rho_{\max}}$$
$$\varepsilon_{low} = 0.0875\rho_{\max} + \frac{6\left(\rho_{srf} - 0.15\rho_{\max}\right)}{0.25\rho_{\max}} \quad \textbf{Eq. 4-7}$$

If Test 1 and Test 2 fail for a certain number of days (i.e., a very bright pixel all the time) then this pixel is assigned to be snow covered. The presented time-series approach is based on the very low temporal variability of snow compared to clouds. Thus, continuously detecting very high reflectivity in one time slot over a certain number of days indicates snow. Problems occur in cases of persistent fog or cloud decks (e.g., marine stratocumulus). In case of a positive snow detection the clear sky reflection is adapted as fast evolution.

The threshold number of days for the snow detection is set to 24. This amount is reduced to 6 in case the considered pixel already had a snow event. This is given by either an amplitude $\rho_{srf} = \rho_{srf,max} - \rho_{srf,min}$ exceeding $0.55\rho_{max}$ or by ρ being larger than a snow threshold ρ_{snow}. The latter is derived empirically so that it is high enough to exclude oceans or other dark surfaces ($\rho_{snow,min}$) and that it favours pixels that have a high ρ_{srf} and thus a higher probability of a former snow event ($\rho_{snow,range}$), see Eq. 4-8.

$$\rho_{snow,\min} = 0.48\rho_{\max}$$
$$\rho_{snow,range} = \max\left(0.15\rho_{\max}, 0.6\rho_{srf,\max}\right) \quad \textbf{Eq. 4-8}$$
$$\rho_{snow} = \max\left(\rho_{snow,\min}, \rho_{srf,\min} + \rho_{snow,range}\right.$$

The calculation of the cloud index n for non-snow pixels follows the standard Heliosat. In case snow is detected the calculation of the cloud index n is altered according to Dürr and Zelenka (2009) in which ρ_{srf} is substituted by $\rho_{snow,min}$ and ρ_{max} is increased by a factor of 1.41 in order to enhance the dynamic range (Eq. 4-9). This altered cloud index formulation generally gives lower cloud index values in order to account for the radiative properties of snow. This includes mainly the reflectivity of the bright snow surface which leads to higher surface radiation values.

$$n = \frac{\rho - 0.48\rho_{\max}}{1.41\rho_{\max} - 0.48\rho_{\max}} = \frac{\rho - 0.48\rho_{\max}}{0.93\rho_{\max}} \quad \textbf{Eq. 4-9}$$

4.2.2.3 Averaging

Monthly, daily and hourly means are calculated by arithmetic averaging, using Eq. 4-10:

$$DAL_{mean} = \frac{\sum_{i=1}^{n} DAL_i}{n} \quad \textbf{Eq. 4-10}$$

Here is a loop over the slots per hour for the calculation of hourly means, a loop over the hourly means for the calculation of the daily means and a loop over daily means for the calculation of monthly means.
SRI is either the i-th daily mean for the calculation of the monthly mean or the i-th hourly mean for the calculation of the daily means. Only the finite values of CAL are summed up, n is the total number of finite values. The larger the number of available images per day, the better the daily cycle of cloud coverage can be resolved, increasing the accuracy of the daily average of SRI. A minimum number of 6 available pixels per day are required to derive the daily mean for this specific pixel. The monthly average is calculated from the daily means of this month on pixel basis as arithmetic mean with a required number of 10 existing daily means.

4.2.3 Atmospheric input information

Here the atmospheric input information used to retrieve daylight is described. The sensitivity of these parameters on the direct irradiance is discussed in section 4.2.4.

Effective cloud albedo and clear sky index:
The effective cloud albedo and clear sky index are derived with the MAGICSOL method; see section 4.2.1 for further details.
The effective cloud albedo is taken from the released CM SAF MVIRI data set (Posselt et al., 2011) and will be calculated from CM SAF GERB/SEVIRI top of atmosphere albedo for the time period covered by SEVIRI.

Aerosol:
Aerosols have a significant effect on the solar irradiance. They scatter and absorb solar radiation. In order to describe the effect of scattering and absorption, information about the aerosol type and aerosol optical depth is needed. The aerosol type determines the relation between scattering and absorption. This relation can be expressed in terms of the single scattering albedo. The asymmetry parameter depends also on the aerosol type (size and composition) and determines the relation between forward- and backward-scattering. However, for the calculation of direct irradiance only the aerosol optical depth is relevant, as the AOD is defined as the attenuation of direct irradiance. The aerosol type and hence the single scattering albedo and asymmetry factor are only of relevance for the total solar irradiance (diffuse + direct irradiance) and thus for the relation between direct and total solar irradiance for a given AOD.
Monthly mean aerosol information is taken from the aerosol climatology by Kinne et al. (2005), which is based on AEROCOM (http://dataipsl.ipsl.jussieu.fr/AEROCOM/) model median and AERONET ground based measurements. This climatology is available in a 1x1 degree resolution and monthly long term means and has been evaluated to outperform the GADS/OPAC climatology (Hess et al., 1998, Köpke et al. 1997) in Africa (Ineichen, 2010).

Please note: Water vapour and ozone does not affect daylight significantly and is therefore not considered.

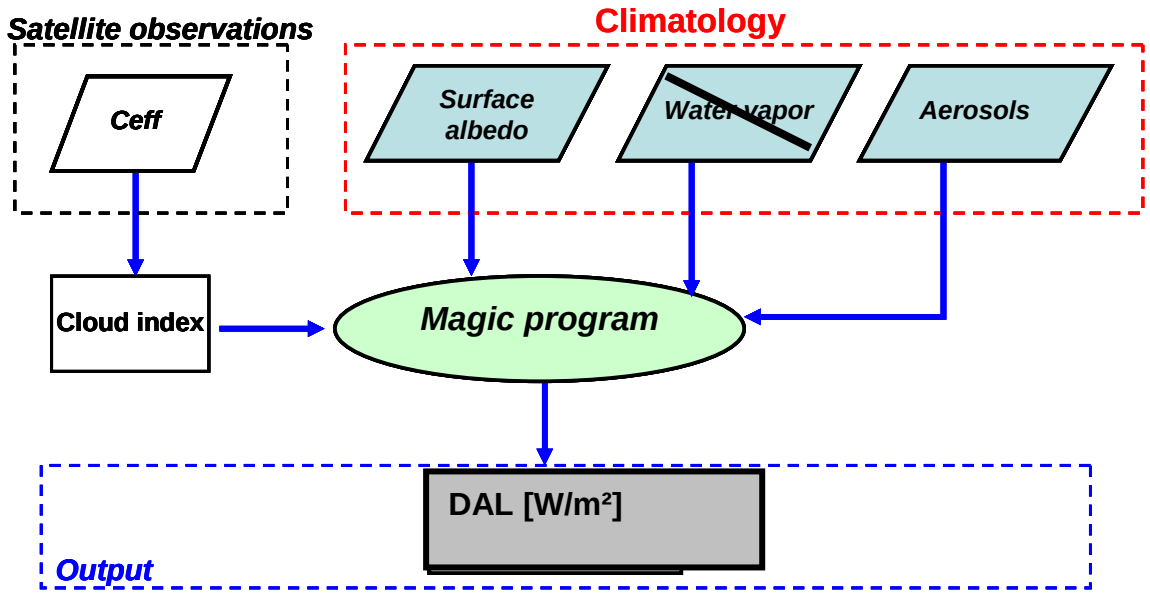

Figure 4–4: Diagram of the interface of MAGIC to the atmospheric input and the satellite observations, Ceff stands for the dark offset corrected and normalised Counts.

4.2.4 Uncertainty estimates

This section provides the uncertainty or sensitivity of Daylight on the clear sky input parameters. The error and accuracy of DAL is assessed by comparison with in-situ data and provided within the validation report. Beside the effect of effective cloud albedo, aerosols have a significant effect on daylight. Water vapour and ozone does not affect daylight significantly attenuation of the solar irradiance, while the surface albedo effect is rather weak. The effective cloud albedo is defined as a relative quantity of observed counts or radiances. Hence, any noise or uncertainty in the satellite observations is predominantly cancelled out. The uncertainty in the effective cloud albedo is therefore pre-dominantly determined by uncertainties in the determination of the clear sky reflection and the self-calibration method.

4.2.4.1 Sensitivity of CAL on self-calibration method

The uncertainty or fuzziness in $\rho_{\max}$ defined by the month to month variations of $\rho_{\max}$ is in the order of 3%. However, it is likely that part of this uncertainty is due to local biases in the satellite counts and not due to errors in the retrieval of $\rho_{\max}$. Local biases of the satellite counts would transfer to equal relative amounts into $\rho_{\max}$ and ρ_{srf}, and would be therefore pre-dominantly cancelled out within the calculation of the effective cloud albedo. Hence, they would not affect the accuracy of CAL. However, as it is not possible do estimate to which amount the local biases counts to the $\rho_{\max}$ uncertainty the complete uncertainty is assumed to arise from the applied statistical retrieval method. This is a worst case approach, since the uncertainty given by the $\rho_{\max}$ retrieval method is likely significantly smaller than 3% and hence also the effect of the $\rho_{\max}$ retrieval method on the accuracy of CAL. The $\rho_{\max}$ uncertainty is constant in terms of relative uncertainty throughout the cloud index interval, but differs in absolute terms in dependency on the surface type. Figure 4–5 shows the effect of a 3 % uncertainty of $\rho_{\max}$ on the effective cloud albedo in absolute values. For a CAL value of 1 the absolute value is equal to the relative uncertainty, which is constant throughout the CAL range.

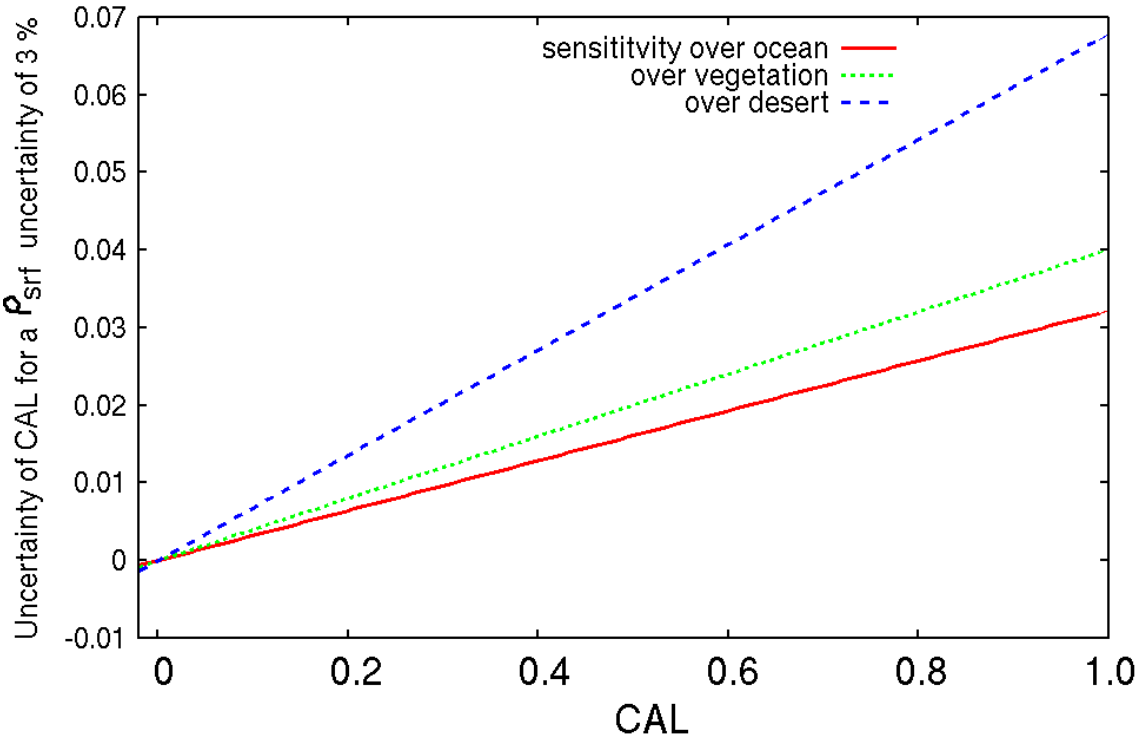

Figure 4–5: Sensitivity of the effective cloud albedo on the ρ_{max} uncertainty for different surface types, with an albedo of 0.05 (~ocean), 0.15 (~vegetation) and 0.35 (~desert).

4.2.4.2 Sensitivity of CAL on clear sky reflection

Figure 4–6 shows the effect on uncertainties in the clear sky reflection on the effective cloud albedo. The effect is rather weak, as a consequence of the occurrence of ρ_{srf} in the dominator and nominator of the effective cloud albedo formula. However, the clear sky reflection introduces significant uncertainty and error in the effective cloud albedo retrieval for the case of cloud contamination. This happens if not enough clear sky cases occur. Hence, for regions with long-lasting cloud cover in combination with slant geometry the ρ_{srf} retrieval fails to see the clear sky situations, hence ρ_{srf} is contaminated by clouds and is artificially increased, see Figure 4–7. This effect occurs pre-dominantly at the border of the MFG disk, above 60 degrees, see Figure 4–8. As it occurs only for regions with long-lasting cloud coverage (hence large values of the effective cloud albedo) the effect on the solar irradiance is much lower as implied by the uncertainty in the effective cloud albedo.

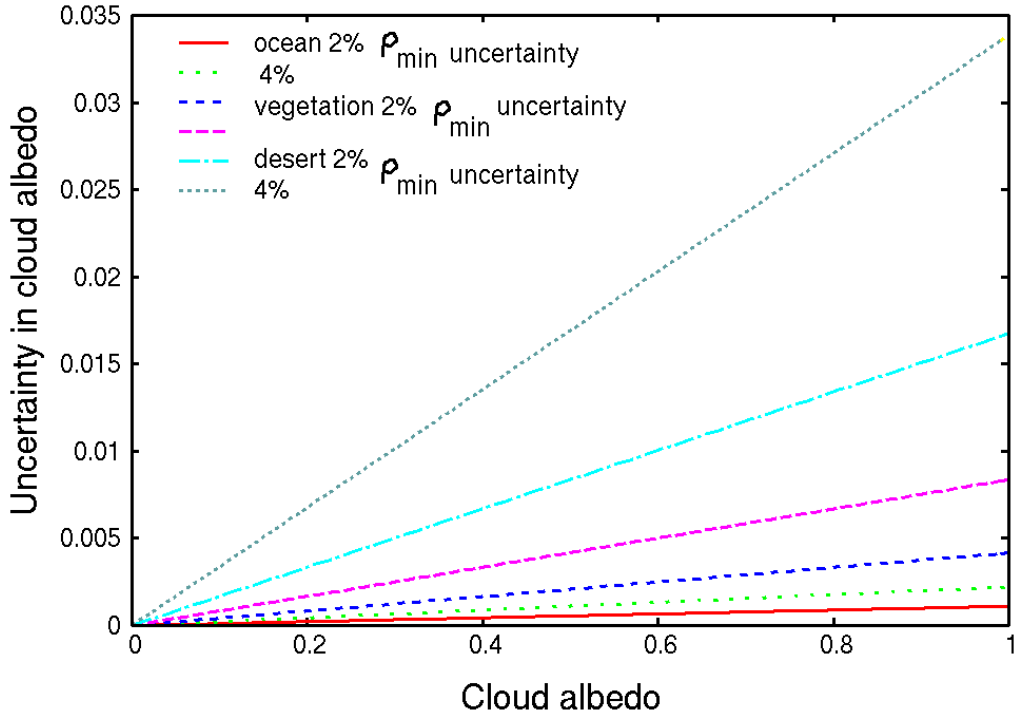

Figure 4–6: Sensitivity of the effective cloud albedo on the clear sky reflection ρ_{srf} in counts. The x-axis compiles the range of the cloud index. On the y-axis the uncertainty or error of the effective cloud albedo is given for different surface types and uncertainties in the retrieval of ρ_{srf} of 2% and 4%, respectively, arising from "statistical noise". The effect of uncertainties of ρ_{srf} on the effective cloud albedo is rather weak. Only for desert (sand) surface an errors in the retrieval of ρ_{srf} would lead to significant errors in the effective cloud albedo.

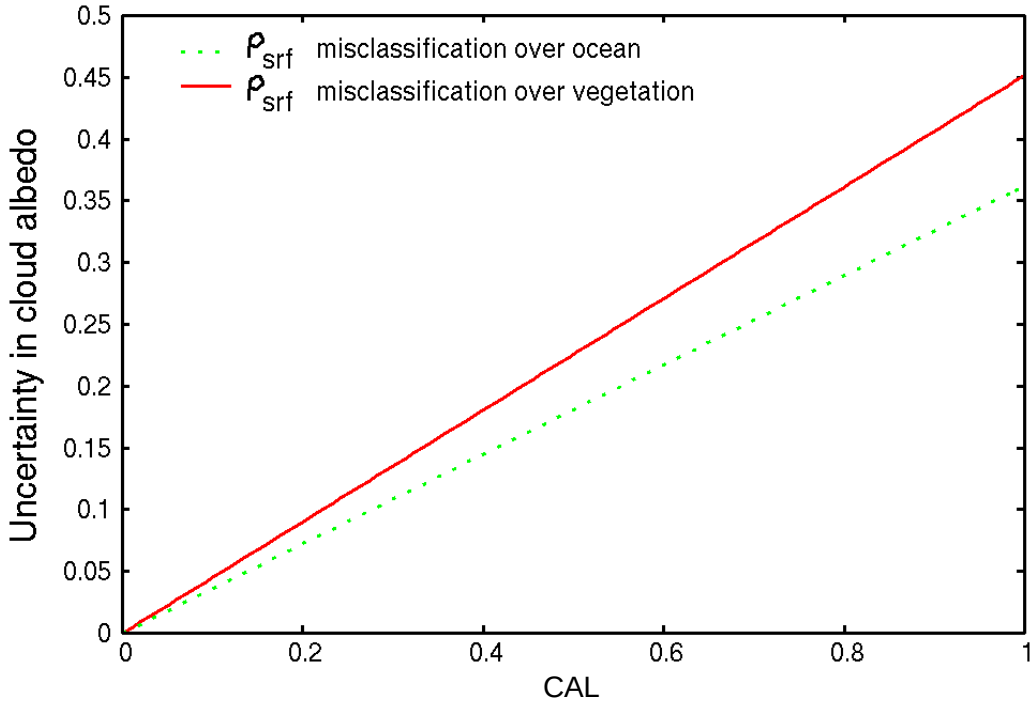

Figure 4–7: Effect of cloud contamination of clear sky reflection on the effective cloud albedo. The effect is rather large. However it occurs pre-dominantly at the border region of the MFG disk. Further on, the effect occurs for long-lasting cloud coverage, the resulting higher uncertainty in the effective cloud albedo has therefore a relative small effect on SIS.

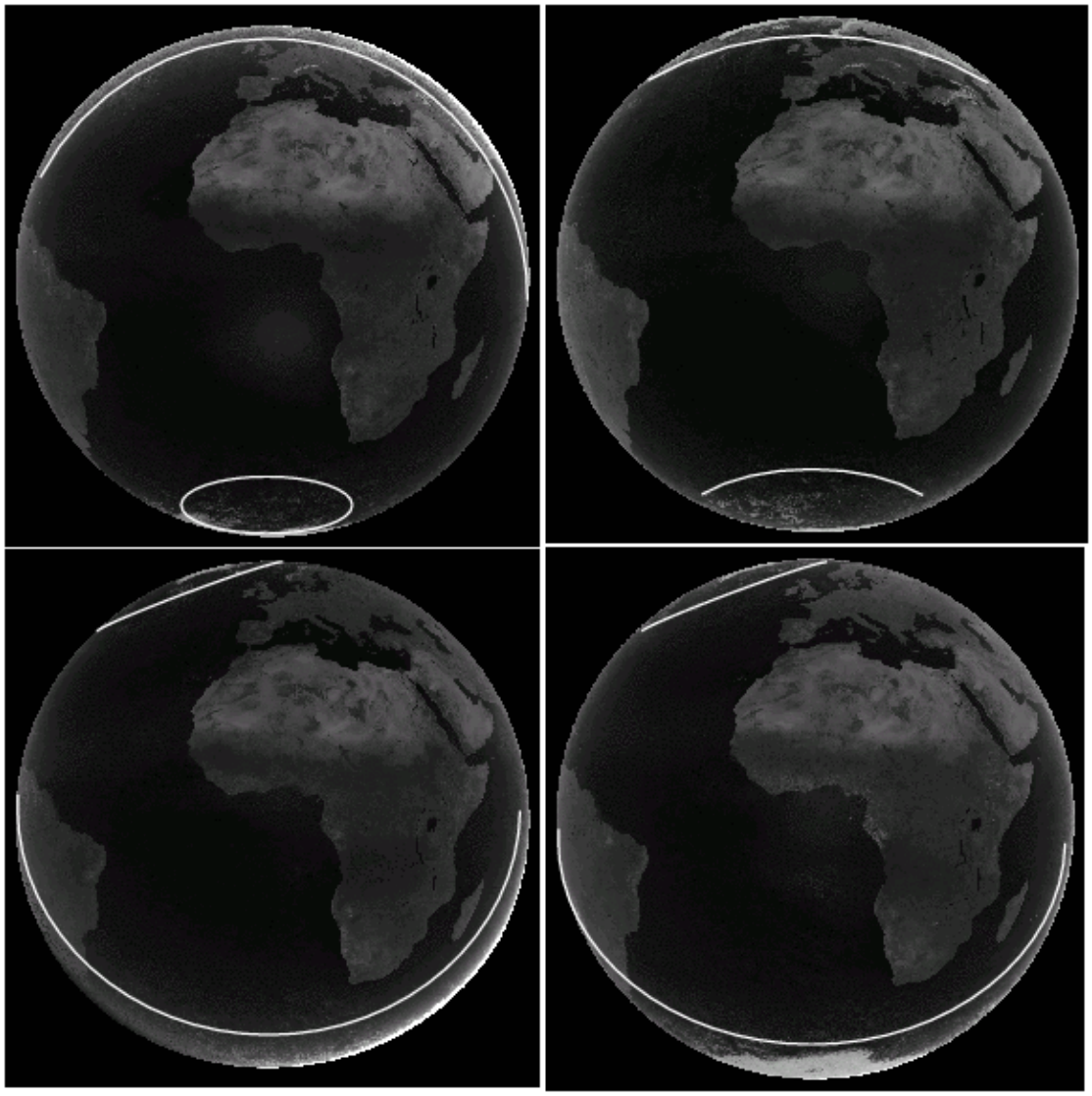

Figure 4–8: Examples of ρ_{sfc} images, here for 2000, 12 GMT, from top left to bottom right, December, March, June and September. The white speckle patterns beyond the white lines close to the border of the disk are due to significant cloud contamination of ρ_{sfc} .However, close to the poles, some white regions are not an artefact bur due to ice (Greenland & Arctic in the September image). Cloud contamination occurs also in a small band around sunrise and sunset at the East and West border of the disk, respectively. However, the core of the Meteosat disk is almost not affected.

4.2.4.3 Water vapour

Table 4-1 shows that DAL is almost not affected by water vapour. Even extreme variations in water vapour from 5 mm to 60mm do only lead to a marginal effect on daylight. The table provides the absolute and relative differences of DAL and SIS for water vapour content of 5 mm and 60 mm for a solar zenith angle of 30 degree and USS standard atmosphere.

Table 4-1: Sensitivity of Daylight and solar surface irradiance SIS for a change of water vapour content from 5mm to 60mm.

Variable	Absolute difference	Relative difference	**Variable**	Absolute Difference	Relative difference
Daylight	0.2 W/m²	0.13 %	**SIS**	102 W/m²	12 %

4.2.4.4 Aerosols

Aerosol type, expressed as single scattering albedo and asymmetry parameter, has a significant effect on the solar irradiance and determines the relation between the diffuse and the direct parts of radiation. The single scattering albedo describes the relation between scattering and absorption, while the asymmetry parameter describes the relation between forward and backward scattering (as a consequence of the particles size). However the attenuation of the direct irradiance by aerosols is completely defined by the AOD, which by definition, describes the attenuation of the direct irradiance. Figure 4–9 shows the sensitivity of daylight on aerosol optical depth and single scattering albedo. It is evident that aerosols do significantly affect daylight.

Typical uncertainties in the monthly mean aerosol optical depth of 0.1 relative to a background of AOD=0.2 leads to uncertainties of about 2 W/m² for maritime and rural aerosols and of about 4 W/m² for aerosol with significant absorbing portion (e.g. urban aerosols).

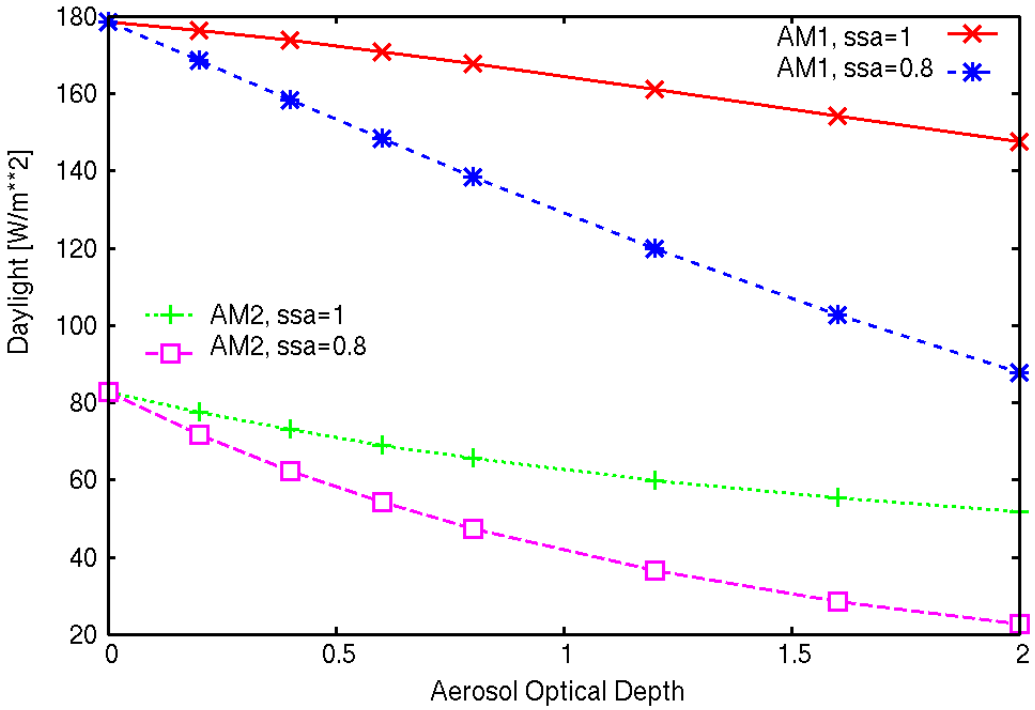

Figure 4–9: Sensitivity of Aerosol optical depth and single scattering albedo (ssa) on daylight for a solar zenith angle of 60 degree (air mass of 2) and 0 degree (AM=1).

4.2.4.5 Surface albedo

Figure 4–10 illustrates the sensitivity of clear sky SIS on uncertainties and errors in the surface albedo. Deviations of +/- 0.1 in the surface albedo lead to deviations in clear sky SIS of +/- 1%. The effect is almost linear. Errors in the surface albedo are expected to be typically less than 0.1, with exception of snow covered surfaces, where higher errors might occur. The effect is pre-dominantly independent on the clear sky atmospheric state.

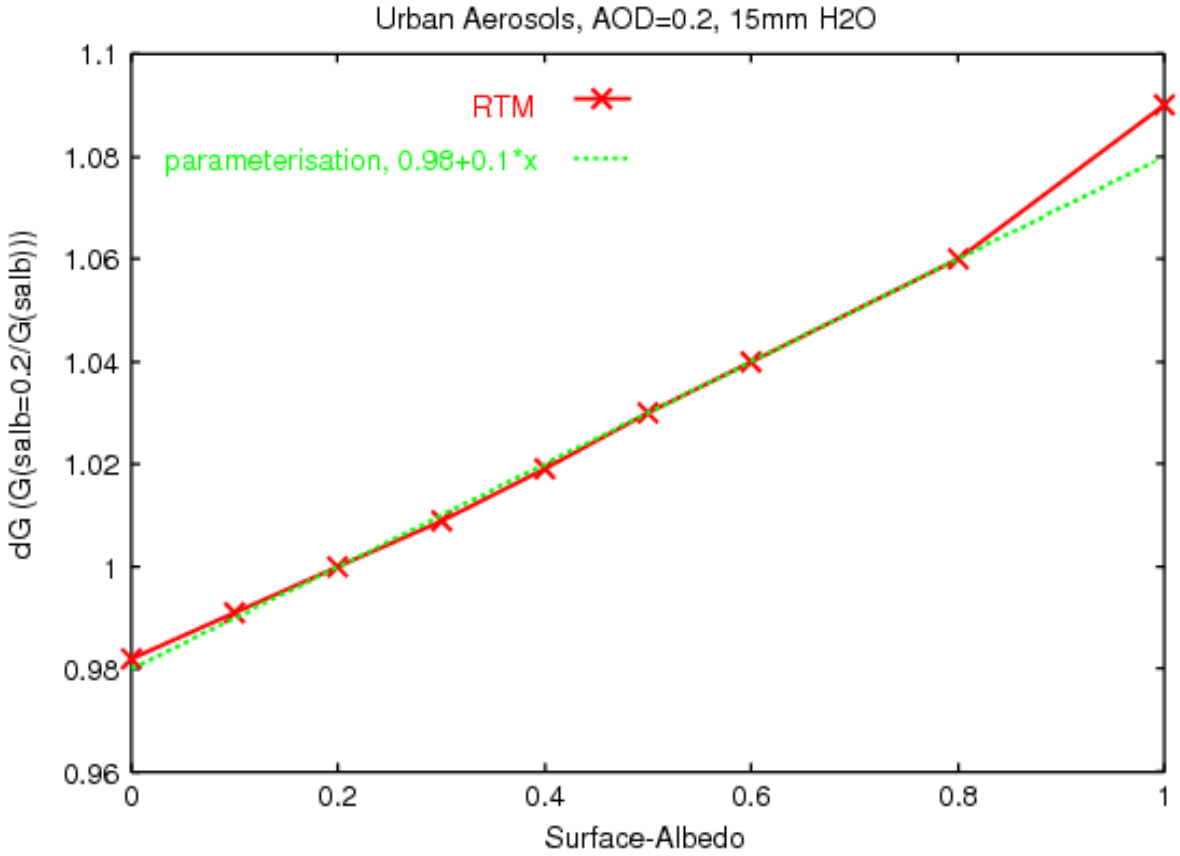

Figure 4–10: Sensitivity of the solar irradiance SIS on the surface albedo. The red line shows the RTM results and the green line the applied parameterisation. The horizontal axis shows the deviation of SIS with variable surface albedo relative to SIS calculated for a fixed surface albedo of 0.2. For deviations of +/- 0.1 in the surface albedo the uncertainty in SIS is +/- 1%. With exception of values above 0.9 the parameterisation matches the RTM results quite well.

4.2.4.6 Effective Cloud albedo

For CAL>0.8 the clouds are rather optical thick and the uncertainty in the solar irradiance is small in absolute terms. Therefore, we focus on the region between 0 and 0.8. Here any uncertainty of CAL in % translates directly in the identical uncertainty in percent for daylight, meaning a 3 % uncertainty in the effective cloud albedo would lead to a 3 % uncertainty in the solar irradiance.

4.3 Practical considerations

The physics of the algorithm follows the MAGICSOL approach which has been successfully applied to retrieve the MVIRI based broadband solar surface irradiance. Hence, it can be expected that the algorithm is able to provide date in appropriate accuracy. Validation results and description of the data will be given in the validation report and product user manual respectively.

5 Assumption, limitations and future improvements

- The high clear-sky reflection over bright surfaces (e.g., desert regions) reduces the contrast between clear-sky reflection and cloudy-sky reflection. This leads to higher uncertainties in CAL and errors in the calculation of SIS. The modified approach for the clear sky reflection improves the accuracy of SIS over bright surfaces, but the accuracy is still significantly lower than for other surfaces.
- In regions with long-lasting cloud cover the modified approach for the clear sky reflection detects snow instead. This results in an underestimation of the effective cloud albedo and errors in the solar irradiance.
- The accuracy of aerosol information is unknown in several regions of the world due to missing ground measurements. Any uncertainty in the aerosol information affects the accuracy of SIS, especially in regions that are dominated by cloudless sky.
- For the calculation of the look-up tables of the clear sky model standard ozone and aerosol profiles are used. These profiles are scaled with the respective vertical column values; see Mayer and Kyling (2005) for further details.
- The USS standard atmosphere has been used to consider the effect of air molecules (e.g. Rayleigh scattering). However, this has no effect on accuracy (Mueller et al, 2009)
- The anisotropy of the cloud reflection leads to uncertainties in the effective cloud albedo and subsequent in the solar surface irradiance. The respective effect is in the order of 1 to 2 % for monthly and daily means respectively. An improved correction of the anisotropy effect will be developed for the next release. However, in general the anisotropy effect is rather small.
- The self calibration method in combination with the modified retrieval of ρ_{srf} is sensitive to significant changes in spectral channels. This implies that using the VIS006 or the VIS008 channel of MSG instead of the broadband channel will lead to significant differences in the effective cloud albedo in specific regions (please see Posselt et al, 2011 for further details). The item is not relevant for the discussed MVIRI climate data sets herein but for the planned prolongation of the record by the use of SEVIRI on board of MSG.

6 References

Betts Alan K., Martin Köhler and Yuanchong Zhang, 2009: Comparison of river basin hydrometeorology in ERA-Interim and ERA-40 reanalyses with observations, Journal of Geophysical Research, Vol. 114, D02101, doi:10.1029/2008JD010761

Beyer, H. G., Costanzo, C., and Heinemann, D.: Modifications of the heliosat procedure for irradiance estimates from satellite images, Solar Energy, 56, 207-212, 1996.

Cano, D., Monget, J. M., Albuisson, M., Guillard, H., Regas, N., and Wald, L.: A method for the determination of the global solar-radiation from meteorological satellite data, Solar Energy, 37, 31-39, 1986.

CIE. (1932). Commission internationale de l'Eclairage proceedings, 1931. Cambridge: Cambridge University Press.

Dagestad, K.-F. (2004), Mean bias deviation of the Heliosat algorithm for varying cloud properties and sun-ground-satellite geometry, Theor. Appl. Climatol. 79, 215–224, DOI 10.1007/s00704-004-0072-5

Dagestad K.-F., J. A. Olseth, A modified algorithm for calculating the cloud index (2007), Solar Energy 81, 280–289.

Derrien,M., LeGLeau, H., 2005: MSG/SEVIRI cloud mask and type from SAFNWC. Int. J. Rem. Sens. 26 (21), 4707 – 4732.

Dürr, B., and Zelenka, A.: Deriving surface global irradiance over the alpine region from meteosat second generation data by supplementing the heliosat method, International Journal of Remote Sensing, 5821-5841, DOI 10.1080/01431160902744829, 2009.

Hammer, A., Heinemann, D., Hoyer, C., Kuhlemann, R., Lorenz, E., Müller, R., and Beyer, H. G.: Solar energy assessment using remote sensing technologies, Remote Sens. Environ., 86, 423--432, 2003.

Hess, M.; P. Köpke; I. Schult, 1998: Optical Properties of Aerosols and Clouds: The Software Package OPAC. Bull. Amer. Meteor. Soc., 79, 831-844.

Kinne, S., M. Schulz, C. Textor et al., 2006, An aerocom initial assessment – optical properties in aerosol component modules of global models, Atmos. Chem. Phys., 6, 1815-1834.

Janjai, S., T. Jantarach, J. Laksanaboonsong, A model for calculating global illuminance from satellite data Renewable Energy 28 (2003) 2355–2365

Krämer, M., Ri. Müller, H. Bovensmann, J. Burrows, J.-U. Grooß, D. S. McKenna, Ro. Müller, Th. Woyke, J. Brinkmann, E.P. Röth, R. Ruhnke, G. Günther, J. Hendricks, E. Lippert, K. S. Carslaw, Th. Peter, A. Zieger, Ch. Brühl, B. Steil and R. Lehmann, 2003: "Intercomparison of Numerical Stratospheric Chemistry Models under Polar Vortex Conditions". Journal of Atmospheric Chemistry, 45, 51-77.

Koepke, P., Bais, A., Balis, D., Buchwitz, M., de Backer, H., de Cabo, X., et al. (1998). Comparison of models used for UV index calculations. Photochemistry and Photobiology, 67, 657−662.
Ineichen, P. “Satellite based short wave irradiance validation over Africa“, Visiting Scientist report of CM-SAF, 2010, available at www.cmsaf.eu.

Kato, S., Ackerman, T., Mather, J., Clothiaux, E., 1999. The k-distribution method and correlated-k approximation for a short-wave radiative transfer. J. Quant. Spectrosc. Radiat. Transfer 62.

Köpke, P.; Hess, M.; Schult, I.; Shettle, E., 1997: Global aerosol data set. Tech. Rep., 243, MPI Meteorology, Hamburg.

Koepke, P., Bais, A., Balis, D., Buchwitz, M., de Backer, H., de Cabo, X., et al. (1998). Comparison of models used for UV index calculations. Photochemistry and Photobiology, 67, 657−662.

Mayer, B.; A. Kylling, 2005: Technical note: “The libRadtran software package for radiative transfer calculations - description and examples of use.” Atmos. Chem. Phys., 5, 1855-1877.

Mayer, B., Seckmeyer, G., & Kylling, A. (1997). Systematic long-term comparison of spectral UV measurements and UVSPEC modeling results. Journal of Geophysical Research, 102, 8755−8767,

Majewski, D., Liermann, D., Prohl, P., Ritter, B. , Buchhold, M., Hanisch, T., Paul,G. Wergen, W. Baumgardner, J., 2002. The Operational Global Icosahedral–Hexagonal Gridpoint Model GME: Description and High-Resolution Tests, Monthly Weather Review, 130, pp 319.

Möser, W. , 1983: Globalstrahlung aus Satellitenmessungen. Mitteilungen aus dem Institut für Geophysik und Meteorologie der Universität zu Köln, 37, Köln.

Müller, R.W.; Dagestad, K.F.; Ineichen, P.; Schroedter-Homscheidt, M.; Cros, S. Dumortier, D.; Kuhlemann, R. ; Olseth, J.A.; Piernavieja, G.; Reise, C.; Wald, L.; Heinemann,D.; 2004: “Rethinking satellite based solar irradiance modelling – The SOLIS clear sky module”, Rem. Sens. Envir., 91, 160-174.

Müller, R.W. et al., 2003-b „Report of the HELIOSAT-3 software package for solar irradiance retrieval, all sky working version” EU report of the Heliosat-3 project (www.heliosat3.de), NNE5-2000-00413

Müller, R.W., Matsoukas, C. Behr, H.D., Gratzki, A. Hollmann, R., 2009: MAGIC - The CM-SAF operational scheme for the satellite based retrieval of solar surface irradiance - a LUT based eigenvector hybrid approach. Remote Sensing of Environment,113, 1012-1024.
Mueller R., Trentmann J., Träger-Chatterjee C., Posselt R., Stöckli R. The Role of the Effective Cloud Albedo for Climate Monitoring and Analysis. *Remote Sensing*. 2011; 3(11):2305-2320.
Posselt R. , Müller R. W., Stöckli R., Trentmann, J. ”Selfcalibration across Meteosat first and second generations”, manuscript in preparation (will be submitted to Remote Sensing: Special Issue "Remote Sensing in Climate Monitoring and Analysis").

Rigollier, C., Lefevre, M., Blanc, P., and Wald, L.: The operational calibration of images taken in the visible channel of the meteosat series of satellites, {J. Atmos. Ocean. Technol.}, {19}, {1285-1293}, 2002.

Skartveit, A., Olseth, J., Tuft, M., 1998: An hourly diffuse fraction model with correction for variability and surface albedo. Solar Energy, **63**, 173–183.

Sharpe, L.T., Stockman, A., Jagla, W., Jägle H. A luminous efficiency function, V*(1), for daylight adaptation, Journal of Vision (2005) 5, 948–968

CIE. (1932). Commission internationale de l'Eclairage proceedings, 1931. Cambridge: Cambridge University Press.

Uppala, S., P. Kallberg, A, Simmons, U. Andreae, V. Da Costa Becthold, M. Firion, J. Gibson, J. Haseler, A. Hernandez, G. Kelly, X. Li, K. Onogi, S. Saarinen, N. Sokka, R. Allan, E. Andersson, E. Arpe, M. Balmaseda, A. Beljaars, L. van de Berg, J. Bidlot, N. Bormann, S. Caires, F. Chevallier, A. Dethof, M. Dragosavac, M. Fisher, M. Fuentes, S. Hagemann, E. Holm, B, Hoskins, L. Isaksen, P. Janssen, R. Jenne, A. McNally, J.-F. Mahfouf, J.J. Morcrette, N. Rayner, R. Saunders, P. Simon, A. Sterl, K. Trenberth, A. Untch, D. Vasiljevic, P. Viterbos, J. Woollen, 2005: The ERA-40 reanalysis. – 436 Quarterly Journal of the Royal Meteorological Society 131, 2961 – 3012.

Van Weele, M., Martin, T., Blumthaler, M., Brogniez, C., den Outer, P., Engelsen, O., et al.(2000). From model intercomparisons towards benchmark UV spectra for six realatmospheric cases. Journal of Geophysical Research, 105, 4915−4925.

Zelenka, A.: Estimating insolation over snow covered mountains with meteosat vis-channel: A time series approach, Proceedings of the Eumetsat Meteorological Satellite Data Users Conference, Eumetsat Publ. EUM P, 2001, 346--352,

Glossary - List of Acronyms in alphabetical order

AVHRR :	Advanced Very High Resolution Radiometer
AOD :	Aerosol Optical Depth
CAL:	Effective cloud albedo
COT	Cloud optical depth
CLS:	CLear Sky
GADS/OPAC:	Global Aerosol Data Set / Optical Properties of Aerosols and Clouds
GERB :	Geostationary Earth Radiation Experiment
k:	Clear sky index.
LUT:	Look-up table
MVIRI :	Meteosat Visible-InfraRed Imager
NOAA :	National Oceanic and Atmospheric Administration
NCEP:	National Centers for Environmental Prediction
RTM:	Radiative Transfer Model
SID:	Surface Direct Irradiance (beam).
SIS:	Solar Surface Irradiance
SZA :	Sun Zenith Angle
SSA:	Single Scattering Albedo